Reconstruction of raster-scanned backscatter x-ray radiography using radial basis functions

Junho Lee [a], Jinwoo Kim [b], Seungjun Yoo [a], Ho Kyung Kim [a,b,*]
[a] *School of Mechanical Engineering, Pusan National Univ., Busandaehakro 63beon-gil, Busan 46241*
[b] *Center for Advanced Medical Engineering, Pusan National Univ., Busandaehakro 63beon-gil, Busan 46241*
[*] *Corresponding author: hokyung@pusan.ac.kr*

1. Introduction

Industrial x-ray non-destructive testing techniques are widely used to detect drugs and explosives at borders [1]. The transmission imaging systems using megavoltage x-ray beams are widely used to provide an internal view of the cargo containers [2], but these deep-penetrating x-ray beams are not suitable for the detection of low-Z materials. In general, low-Z materials such as drugs, bullets, and plastic guns are inspected using backscatter x-ray imaging (BXI) systems, which utilize more soft x-rays in kilovoltage ranges [3]. Typical BXI systems employ collimator wheels for pencil-beam irradiation and a set of large-area scintillation detectors to detect backscattered x-ray photons [4]. The x-ray beam irradiates the vehicle vertically using a collimator wheel while the vehicle moves horizontally. Therefore, the reconstructed raster-scanned images cannot avoid geometric distortion due to the nonuniform vertical sampling pitches, which is originated from the mismatch of the rotation speed of the collimator wheel and the translation speed of the vehicles. The distortion becomes more severe when the moving speed of the vehicle becomes faster than the angular velocity of the collimator wheel. A robust image reconstruction algorithm that minimizes these distortions can provide a large improvement in the efficiency of the BXI systems in terms of reliability and speed of inspection.

In this study, we propose a radial-basis function (RBF)-based interpolation method for the reconstruction of BX images. The proposed method can reduce distortions on the reconstructed BX images by a nonlinear interpolation for nonuniformly distributed backscattered signals. The performance of the proposed method is investigated for various combinations of Gaussian basis functions.

2. Methods

2.1 Geometric distortion due to the raster-scanning

The BXI systems generally employ a raster-scanning geometry as shown in Fig. 1. The trajectory of the incident x-rays on the surface of the vehicle is mainly determined by the angular velocity of the collimator wheel ω and the vehicle speed v_x. The trajectory follows the tangential function since the x-rays from the rotating collimator wheel are emitted for each specific angular interval, while the vehicle is moving at a constant velocity. As a result, the y-directional sampling pitch decreases rapidly from the top point, approaches the minimum value, and then increases again. Fig. 2 shows

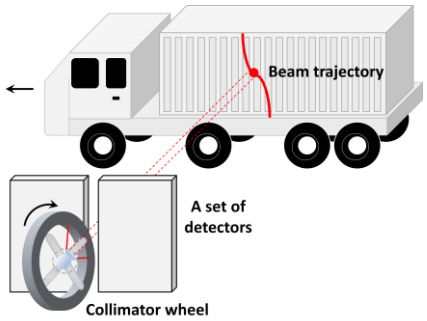

Fig. 1. A schematic diagram for describing raster-scanning geometry for typical BXI systems.

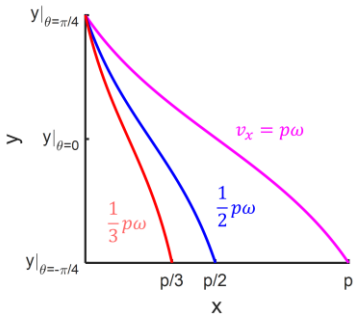

Fig. 2. The beam trajectories for several v_x for a fixed ω. p denotes x-directional sampling pitch of raster scanning.

the examples of the beam trajectory for several v_x for a fixed ω.

2.2 RBF-based interpolation

An RBF-based interpolation method is a powerful tool for interpolating scattered data [5]. Scattered data are approximated by a linear combination of radial basis functions. In this study, the 2-D Gaussian basis functions for a wide range of standard deviations are used to reconstruct the backscattered x-ray images:

$$g(x,y) = e^{-\frac{(x-x_0)^2}{2\sigma_x^2}-\frac{(y-y_0)^2}{2\sigma_y^2}}. \quad (1)$$

For a given set of coordinates $\mathbf{p} = [p_1, p_2, \ldots, p_n]$ and intensities $\mathbf{I} = [I_1, I_2, \ldots, I_n]$ of scattered data, the weights $\boldsymbol{\lambda} = [\lambda_1, \lambda_2, \ldots, \lambda_n]$ of each Gaussian basis function can be obtained by applying conjugate gradient method:

$$\begin{bmatrix} g(\|p_1-p_1\|) & \cdots & g(\|p_n-p_1\|) \\ \vdots & \ddots & \vdots \\ g(\|p_1-p_n\|) & \cdots & g(\|p_n-p_n\|) \end{bmatrix} \begin{bmatrix} \lambda_1 \\ \vdots \\ \lambda_n \end{bmatrix} = \begin{bmatrix} I_1 \\ \vdots \\ I_n \end{bmatrix}. \quad (2)$$

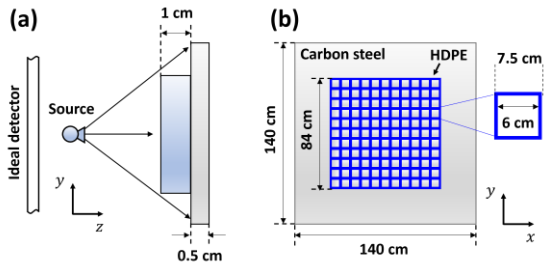

Fig. 3. Monte Carlo simulation geometry for BXI system: (a) side view and (b) rear view.

Then the intensity for an arbitrary coordinate is approximated by a combination of the weighted basis functions:

$$I = \lambda_1 g(\|p_1 - p\|) + \cdots + \lambda_n g(\|p_n - p\|). \quad (3)$$

2.3 Monte Carlo evaluation

The Monte Carlo (MC) simulations are performed to acquire backscatter signals for a typical BXI geometry. All the simulations are performed by the commercial MC radiation transport code (MCNP version 5, RSICC, Oak Ridge, TN). Fig. 3 shows the MC geometry for the BXI simulations. A computational phantom composed of an 84 × 84 cm^2-sized rectangular lattice-structured high-density polyethylene and a 140 × 140 cm^2-sized carbon steel plate is scanned for v_x = 0.5 cm/s and 1.0 cm/s, while ω is fixed to a constant value of $\frac{\pi}{2}$ rad/s. The distance between source and object is set to 63.75 cm and a 600 × 600 cm^2-sized ideal surface detector to tally the energy of backscattered x-ray photons is located right behind the source.

The tallied signals are reconstructed using RBF-based and bilinear interpolation methods. The performances of both methods are quantitatively evaluated by calculating normalized mutual information (NMI) [6] between reconstructed raster-scanned images and the ground truth images.

$$\mathrm{NMI}(\mathbf{x},\mathbf{y}) = \frac{H(\mathbf{x})+H(\mathbf{y})-H(\mathbf{x},\mathbf{y})}{\sqrt{H(\mathbf{x})H(\mathbf{y})}}, \quad (4)$$

where $H(\mathbf{x})$ and $H(\mathbf{x},\mathbf{y})$ denote the entropy of an image **x** and joint entropy of **x** and **y**, respectively.

3. Preliminary Results

The NMI values obtained from RBF-based and bilinear interpolations are summarized in Tab. I. For v_x = 0.5 cm/s, the Gaussian RBF-based interpolation shows high NMI values for the ranges of $0.25 \le \sigma_x \le 0.5$ and $0.25 \le \sigma_y \le 0.5$, while the best NMI values are observed in the range of $0.5 \le \sigma_x \le 1.0$ and $0.25 \le \sigma_y \le 0.5$ for v_x = 1.0 cm/s. This observation shows that the x-directional width of the Gaussian basis function should be enlarged for the high translation speed conditions. The optimal range of σ_y is not changed since the y-directional sampling pitch was kept constant for both cases. Fig. 4 compares the raw and interpolated BX images for v_x = 0.5 cm/s. The raw image seems to be vertically stretched due to the nonuniform y-directional sampling pitches.

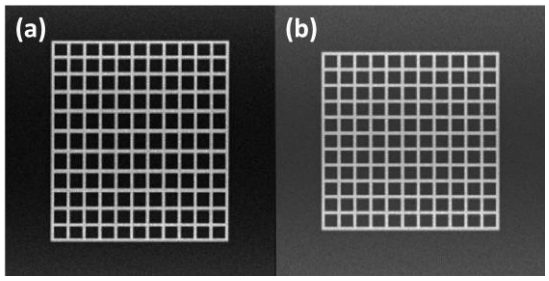

Fig. 4. Comparison of (a) raw and (b) RBF-based interpolated BX images for v_x = 0.5 cm/s.

4. Conclusion

An RBF-based nonlinear interpolation method to minimize the distortion of BX images has been introduced. The proposed method was evaluated for a BX image reconstruction of the lattice-structured computational phantom using MC simulations. The preliminary results show that there are optimal basis functions for a specific scan condition. Our future study includes a more quantitative analysis for various radial basis functions and phantoms.

ACKNOWLEDGEMENTS

This work was conducted as a part of the research projects of "Development of automatic screening and hybrid detection system for hazardous material detecting in port container" financially (20200611) supported by the Ministry of Oceans and Fisheries, Korea.

REFERENCES

[1] G. Zentai, X-Ray Imaging for Homeland Security, International Journal of Signal and Imaging Systems Engineering, Vol. 3, No. 1, pp. 13-20, 2010.
[2] H. E. Martz, Jr., S. M. Glenn, J. A. Smith, C. J. Divin, and S. G. Azevedo, Poly- Versus Mono-Energetic Dual-Spectrum Non-Intrusive Inspection of Cargo Containers, IEEE Transactions on Nuclear Science, Vol. 64, No. 7, pp. 1709-1718, 2017.
[3] J. Callerame, X-ray Backscatter Imaging: Photography Through Barriers, Powder diffraction, Vol. 21, No. 2, pp. 132-135, 2006.
[4] S. Kolkoori, N. Wrobel, K. Osterloh, U. Zscherpel, and U. Ewert, Novel X-ray Backscatter Technique for Detection of Dangerous Materials: Application to Aviation and Port Security, Journal of Instrumentation, Vol. 8, No. 09, pp. P09017
[5] V. Skala, RBF Interpolation with CSRBF of Large Data Sets, Procedia Computer Science, Vol. 108, pp. 2433-2437, 2017.

[6] A. Strehl and J. Gosh, Cluster Ensembles---A Knowledge Reuse Framework for Combining Multiple Partitions, Journal of Machine Learning Research, Vol. 3, pp. 583-617, 2002

Tab. I. Summary of calculated NMI values for the various combinations of the x- and y-directional standard deviations of the Gaussian basis function.

v_x (cm/s)	0.5				1.0			
σ_y (cm) \ σ_x (cm)	0.25	0.5	1.0	1.5	0.25	0.5	1.0	1.5
0.25	0.1399	0.1380	0.0236	0.0084	0.0697	0.1305	0.1280	0.1097
0.5	0.1468	0.1378	0.0257	0.0097	0.0709	0.1375	0.1294	0.1004
1.0	0.0218	0.0198	0.0110	0.0060	0.0197	0.0234	0.0204	0.0426
1.5	0.0082	0.0106	0.0097	0.0048	0.0090	0.0052	0.0130	0.0156